

# Long-range electron tunnelling in oligo-porphyrin molecular wires

Gita Sedghi<sup>1</sup>, Víctor M. García-Suárez<sup>2,3</sup>, Louisa J. Esdaile<sup>4</sup>, Harry L. Anderson<sup>4\*</sup>, Colin J. Lambert<sup>2\*</sup>, Santiago Martín<sup>1,5</sup>, Donald Bethell<sup>1</sup>, Simon J. Higgins<sup>1</sup>, Martin Elliott<sup>6</sup>, Neil Bennett<sup>6</sup>, J. Emyr Macdonald<sup>6</sup> and Richard J. Nichols<sup>1\*</sup>

**Short chains of porphyrin molecules can mediate electron transport over distances as long as 5–10 nm with low attenuation. This means that porphyrin-based molecular wires could be useful in nanoelectronic and photovoltaic devices, but the mechanisms responsible for charge transport in single oligo-porphyrin wires have not yet been established. Here, based on electrical measurements of single-molecule junctions, we show that the conductance of the oligo-porphyrin wires has a strong dependence on temperature, and a weak dependence on the length of the wire. Although it is widely accepted that such behaviour is a signature of a thermally assisted incoherent (hopping) mechanism, density functional theory calculations and an accompanying analytical model strongly suggest that the observed temperature and length dependence is consistent with phase-coherent tunnelling through the whole molecular junction.**

Charge transport in oligo-porphyrins can be probed by direct electrical measurements<sup>1–4</sup> or by photo-induced electron transfer<sup>5–7</sup>. In the former, the oligo-porphyrin is attached to two electrodes, typically metals, and charge flow through the molecular wire is measured. In the latter, the oligo-porphyrin forms a bridge between donor and acceptor moieties, and charge transfer dynamics are probed using photo-physical methods. Time-resolved microwave conductivity can also be used to probe the flow of charge through a molecular wire without the need for metal electrodes<sup>1–3,5,8</sup>. All three methods show oligo-porphyrins to be capable of efficient long-range charge transport. Developments in scanning tunnelling microscopy (STM) have made it possible to place single porphyrin molecules between an STM tip and a metal surface, and to measure either the conductance or current–voltage characteristic of the molecular bridge<sup>1,4</sup>. Gold–thiol linkages have been used to bind porphyrin oligomers within an electrical junction in an STM, and to quantify the low-bias conductance of a homologous series of oligo-porphyrins (which consisted of one, two and three porphyrin moieties, connected through butadiyne linkers to retain good conjugation along the oligomer). The weak decay of conductance as a function of length attested to their effective long-range charge transport properties<sup>1</sup>. Subsequently an STM break-junction technique was used to demonstrate that the position of the thiol linkers on the porphyrin ring can influence the efficacy with which gold–porphyrin–gold junctions are formed<sup>4</sup>. However, the mechanisms responsible for charge transport in these single-molecule junctions with porphyrin wires remain elusive, and it is not clear if coherent or incoherent process are involved.

It is often assumed that low values of the attenuation factor  $\beta$  (for example,  $\beta = (0.040 \pm 0.006) \text{ \AA}^{-1}$  is reported in ref. 1) indicate an incoherent hopping transport mechanism, on the grounds that these  $\beta$  values must correspond to barrier heights of less than the thermal energy at room temperature. However, simple relationships between barrier height ( $\Phi$ ) and  $\beta$ , such as  $\beta = 1.02 \times \Phi^{1/2}$ , where  $\beta$

is in  $\text{\AA}^{-1}$  and  $\Phi$  is in eV (see, for example, ref. 9), are too crude an approximation, because they assume a free electron mass, a simple rectangular barrier and, importantly, a barrier that is independent of length. As we will show here, ultralow attenuation factors can be consistent with phase-coherent tunnelling and do not necessarily imply such low barrier heights. The unusually low attenuation of these oligo-porphyrins and the fundamental question about the mechanism of conductance in such wires have prompted us to investigate the temperature dependence of electron transport, using a combination of experimental measurements and first-principles theory.

Temperature variation has been widely used in organic electronics<sup>10</sup>, because it is relatively straightforward to cool a bulk organic device from ambient to low temperatures while monitoring the current–voltage characteristic. In molecular electronics, where relatively small numbers of molecules or even single molecules are attached to electrodes, variable temperature has been used less routinely. Conducting atomic force microscopy (AFM) has been used to measure the temperature-dependent conductance of conjugated oligomers in self-assembled monolayers, sandwiched between a gold surface and gold-coated AFM tip<sup>11,12</sup>. Longer oligomers showed thermally activated charge transport, which was quantified through Arrhenius-type plots, whereas shorter oligomers showed a temperature-independent behaviour attributed to tunnelling<sup>11,12</sup>. In earlier pioneering experiments, molecular junctions involving a small number of molecules have been formed between electrodes defined by electron-beam lithography<sup>13</sup>. It was shown that charge transport in such junctions could undergo a transition from tunnelling to incoherent thermally assisted hopping. A transition from temperature-independent to temperature-dependent conductance with increasing temperature has also been observed in three-terminal molecular devices formed by electromigration<sup>14</sup>. This was attributed to the temperature dependence of the Fermi distribution in the leads<sup>14</sup>. However, single-molecule break-junction techniques,

<sup>1</sup>Chemistry Department, University of Liverpool, Liverpool L69 7ZD, UK, <sup>2</sup>Department of Physics, Lancaster University, Lancaster LA1 4YB, UK, <sup>3</sup>Departamento de Física, Universidad de Oviedo & CINN, 33007 Oviedo, Spain, <sup>4</sup>Department of Chemistry, University of Oxford, Chemistry Research Laboratory, Mansfield Road, Oxford OX1 3TA, UK, <sup>5</sup>Departamento de Química Física, Universidad de Zaragoza & INA, 50009 Zaragoza, Spain, <sup>6</sup>School of Physics and Astronomy, Cardiff University, Cardiff CF24 3AA, UK. \*e-mail: nichols@liverpool.ac.uk; harry.anderson@chem.ox.ac.uk; c.lambert@lancaster.ac.uk

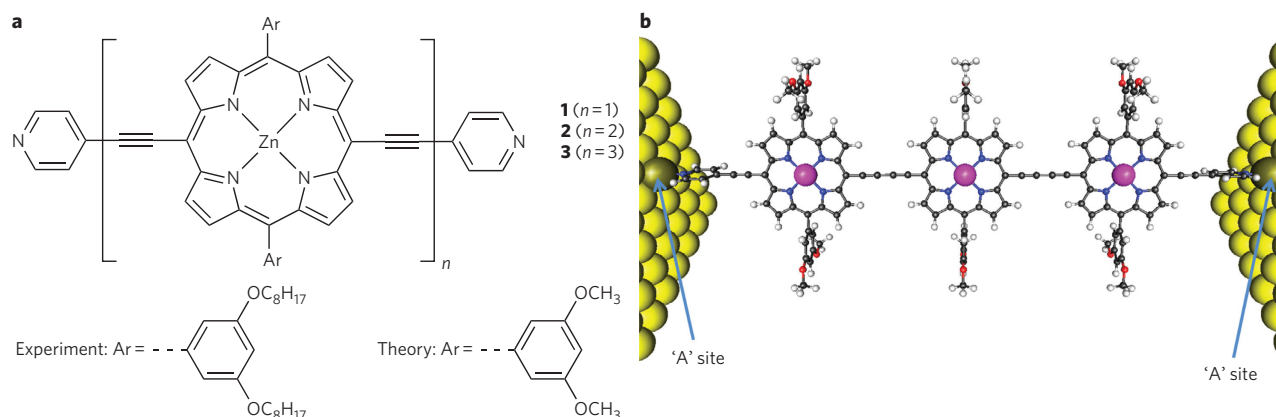


**Figure 1 | Structure of the oligo-porphyrins.** **a**, Compounds  $n=1$  (monomer),  $n=2$  (dimer) and  $n=3$  (trimer). The  $C_8H_{17}O$  pendent side chains in compounds 1–3 are replaced by  $H_3CO-$  side chains in the structural model. **b**, Schematic representation of the butadiyne-linked trimer between gold leads, when the porphyrin rings lie in one plane. Axial ligands (pyridine) binding to the Zn centres are also not shown (these inhibit aggregation of the molecules and are observed to promote the formation of Au | oligoporphyrin | Au junctions in the STM experiments). The terminal N atoms are bonded to gold adatoms on each electrode surface (A–A configuration). Atom colouring: C, dark grey; H, light grey; N, blue; O, red; Zn, pink; Au, yellow.

which use either an STM or a mechanically controlled break-junction, have less frequently applied variable temperature to analyse transport mechanisms<sup>15–19</sup>. An example of such measurements is the observation of temperature dependence for redox-active perylene tetracarboxylic dimide, which was taken as proof of a thermally activated two-step sequential process<sup>18</sup>. In what follows, we use variable-temperature STM to study the conductance of oligo-porphyrin single-molecule junctions, and we examine the conduction mechanisms with both an analytical model and *ab initio* transport computations based on density functional theory (DFT).

### Single-molecule conductance of oligo-porphyrins

A homologous series of oligo-porphyrins, with one, two and three porphyrin units, has been examined (oligomers 1–3 in Fig. 1a). Figure 1b shows a schematic representation of the butadiyne-linked trimer between gold leads, with the porphyrin rings lying in one plane. The porphyrins are connected by butadiyne linkers to promote electronic conjugation along the oligomer, and terminal pyridine groups enable the wires to be linked to the gold contacts. These pyridyl terminals have been found to be effective for contacting gold electrodes<sup>20–28</sup>. Pyridine was also used as a ligand, binding in an axial position to the metal core of the porphyrin; in its absence it was difficult to achieve well-defined molecular junctions, suggesting that it hampers direct interaction of the porphyrin rings and gold contacts as well as molecular aggregation (see Supplementary Information). Single-molecule conductance was determined using the  $I(s)$  technique, which uses an STM to form molecular bridges between a gold tip and a gold substrate surface<sup>23,29–31</sup>. The term  $I(s)$  refers to the measurement of the current  $I$  as the molecules are extended by a distance  $s$  in the STM junction (see Methods). These  $I(s)$  curves are statistically analysed in histograms to give the junction conductance.

The inset of Fig. 2a shows a selection of current–distance curves for porphyrin 2 (the dimer). As the STM tip is retracted in the  $I(s)$  experiment, a plateau is observed, with the target porphyrin bridging between the STM tip and the substrate surface. The tip is retracted until this molecular junction breaks, as indicated by a sharp drop in the current at the break-off distance. Many  $I(s)$  curves are analysed statistically to produce conductance histograms, which use in their construction all current values from the collected  $I(s)$  curves. A room-temperature conductance histogram is shown in Fig. 2a for porphyrin 2 (histograms for monomer 1 and trimer 3 are shown in the Supplementary Information). Fitting the molecular

conductance  $\sigma_M$  versus bridge length  $s_M$  to an exponential decay ( $\sigma_M \propto e^{-\beta s_M}$ ) for this homologous series gives a very low attenuation factor,  $\beta = (0.040 \pm 0.006) \text{ \AA}^{-1}$ , which attests to the very shallow length dependence of the conductance. Similar behaviour has been reported previously for analogous compounds<sup>1</sup>, but with thiol end groups rather than the pyridyl groups used in this study. This demonstrates that the low attenuation of the oligo-porphyrin bridges remains, even with substantially different linking of these molecular wires to the metal leads. However, as discussed in the Supplementary Information, the length dependence alone provides no definitive indication of the mechanism of charge transport through these molecular wires. We therefore turn our attention to an analysis of the temperature dependence of molecular conductance.

There have been a number of studies of the temperature dependence of the conductivity or photoconductivity of metalloporphyrin bulk films<sup>32,33</sup>, bulk materials consisting of metallic nanoparticles interconnected by oligoporphyrin linkers<sup>34</sup> and long porphyrin arrays<sup>2</sup>. Charge transport in single-molecule wires is a distinctly different subject to charge transport in bulk films (see, for instance, a discussion of the differences between conductance in mesoscopic wires, bulk conducting polymers and oligomers of polyaniline<sup>35</sup>). There have been no studies of single-molecule conductance of short porphyrin oligomers formed in molecular break-junctions over a range of temperatures. In the present study, we take the approach of determining the temperature dependence of single-molecule junctions analysed with conductance histograms statistically generated from a large number of junction formation cycles. These will be free from bulk or ensemble effects, allowing us to examine the intrinsic conduction mechanism of the porphyrin oligomers. We have carried out single-molecule conductance measurements at elevated temperatures by recording  $I(s)$  traces with the gold samples mounted on a metal plate heated with a variable-temperature resistive heating source. Using this temperature control system, single-molecule conductance was determined for compound 2 in the temperature range 25–100 °C using the same histogram analysis as was used for the room-temperature measurements. Statistically generated conductance histograms recorded over a range of temperature are shown in Fig. 2b. There is a marked dependence of the peak position on temperature, indicating thermal activation of the transport. Such behaviour is conventionally taken as indicating transport by thermally activated incoherent hopping, which is why we plot the data in Arrhenius form (inset to Fig. 2b). We have performed similar variable-temperature single-molecule

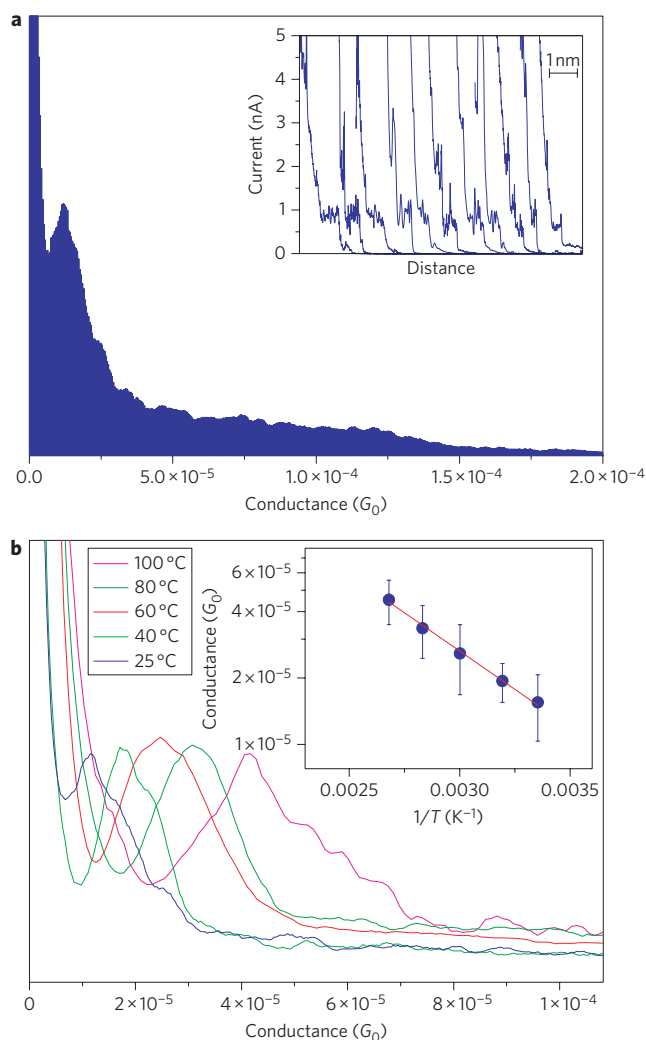


**Figure 2 | Single-molecule conductance data for the dimer.** **a**, Conductance histogram and  $I(s)$  curves (inset) for porphyrin **2** recorded by an STM at room temperature, with  $V_{\text{bias}} = 0.6$  V and a set point current of 6 nA. A total of 285  $I(s)$  curves are included in the histogram. **b**, Conductance histograms for porphyrin dimer **2** at five different temperatures. Inset: Arrhenius-type plot of the single-molecule conductance  $\sigma$ . The red line is the best fit to the data points, and error bars refer to one standard deviation of the data points forming the histogram peak (from its mean value).

conductance measurements for **1** (monomer) and **3** (trimer). The respective slopes of the Arrhenius plots are  $-950$   $\text{K}^{-1}$  (0.08 eV, monomer),  $-1,600$   $\text{K}^{-1}$  (0.14 eV, dimer) and  $-2,600$   $\text{K}^{-1}$  (0.22 eV, trimer).

### Mechanisms of charge transport

On first examination, interpretation of the temperature-dependent transport for the porphyrin single-molecule wires within a hopping-type model may seem attractive. The clear identification of hopping sites is not necessarily obvious, because in such a description the activation barrier may be associated with a loosely defined subsection of the molecule. Within the simplest models, potential hopping sites could be considered to be monomeric units within the oligomer or they could involve two (for the dimer) or three (for the trimer) electronically connected porphyrin units. Incoherent transport may then proceed by ionization and neutralization of these sites or by the formation of polarons. However, this would imply a decreasing temperature dependence in moving from the monomer to the trimer, provided the activation

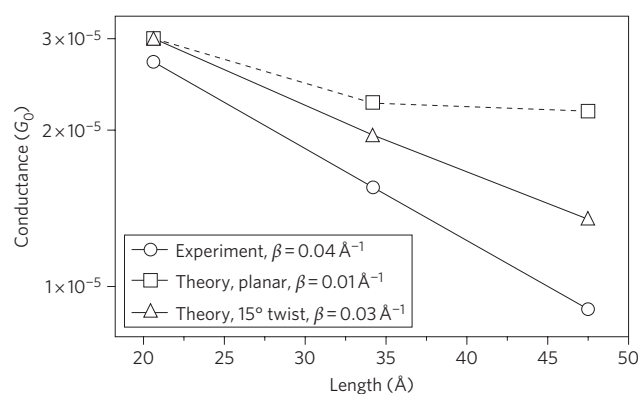


**Figure 3 | Dependence of conductance of oligo-porphyrins on length.**

Conductance data at 25 °C for the monomer, dimer and trimer (open circles). Theoretical data are also shown for when the dihedral angle between the rings is  $0^\circ$  (squares) and  $15^\circ$  (triangles). The theoretical values were calculated with a single-zeta basis set in the leads and a double-zeta polarized basis set in the molecule. The coupling nitrogen atoms at each end of the molecular bridge were located on top of a gold adatom and the leads were grown along the (001) direction of fcc gold, with 49 atoms per slice. The conductance values were evaluated by taking the transmission near the HOMO resonance (see text). The y-scale is logarithmic. Straight lines are plotted to connect points.

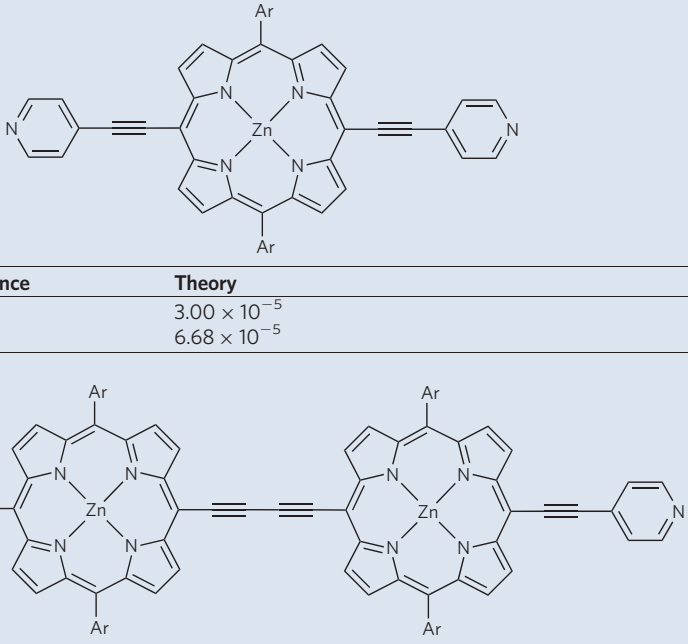
barrier is identified with the decreasing gap between the highest occupied molecular orbital (HOMO) and the lowest unoccupied molecular orbital (LUMO). Experimentally, the opposite is observed, with the temperature dependence of the conductance increasing significantly from monomer to dimer and then to trimer. The transport behaviour does not therefore readily fit a simple hopping model, and in the following we show that this trend is instead consistent with phase-coherent tunnelling.

Although a pronounced temperature dependence and slow decay of molecular conductance with length of the molecular wire are commonly taken as signatures of hopping, it is recognized that coherent tunnelling can also lead to pronounced temperature dependence of the conductance (see, for example, the discussion in ref. 10). The temperature dependence of the conductance can be large when coherent transport takes place on resonance<sup>10,14</sup>. On the other hand, far off-resonance, where the energy dependence of the transmission coefficient is not pronounced, molecular conductance can be almost temperature-independent. For example, in molecular junctions containing tercyclohexylidene molecular wires with thiol end groups, the increasing conductance observed at sufficiently high temperatures has been attributed to the temperature dependence of the Fermi distribution function of the leads, within a simple resonant tunnelling model<sup>14</sup>.

For coherent tunnelling at temperature  $T$  and bias  $V$ , the current  $I$  and conductance  $G$  can be calculated by integrating the electron transmission coefficient  $T(E)$  with energy  $E$ :

$$G(V, T) = \frac{I(V, T)}{V} = \frac{2e}{h} \int_{-\infty}^{\infty} dE T(E) \frac{f(E - E_F - eV/2, T) - f(E - E_F + eV/2, T)}{V} \quad (1)$$

where  $f(x, T) = (\exp x/k_B T + 1)^{-1}$  is the Fermi function,  $k_B$  is Boltzmann's constant,  $e$  is the electron charge and  $E_F$  is the Fermi energy. The transmission coefficient  $T(E)$  can be determined from *ab initio* DFT calculations, for example. The Fermi function gives rise to a temperature dependence of the current<sup>10,14</sup>, even in the

**Table 1 | Calculated and measured values of the conductance for the monomer, dimer and trimer (in units of  $G_0$ ) for various values of the dihedral angle  $\varphi$  between adjacent porphyrin rings and the temperatures.**


$T$ (°C)	Experimental conductance	Theory
25	$2.71 \times 10^{-5}$	$3.00 \times 10^{-5}$
100	$5.17 \times 10^{-5}$	$6.68 \times 10^{-5}$

$T$ (°C)	Experimental conductance	Theory ( $\varphi = 0^\circ$ )	Theory ( $\varphi = 15^\circ$ )	Theory ( $\varphi = 90^\circ$ )
25	$1.55 \times 10^{-5}$	$2.26 \times 10^{-5}$	$1.96 \times 10^{-5}$	$4.44 \times 10^{-10}$
100	$4.52 \times 10^{-5}$	$4.26 \times 10^{-5}$	$3.80 \times 10^{-5}$	$4.77 \times 10^{-9}$

$T$ (°C)	Experimental conductance	Theory ( $\varphi = 0^\circ$ )	Theory ( $\varphi = 15^\circ$ )	Theory ( $\varphi = 90^\circ$ )
25	$9.04 \times 10^{-6}$	$2.18 \times 10^{-5}$	$1.35 \times 10^{-5}$	$2.60 \times 10^{-11}$
80	$3.88 \times 10^{-5}$	$3.01 \times 10^{-5}$	$2.04 \times 10^{-5}$	$2.02 \times 10^{-10}$
100		$3.30 \times 10^{-5}$	$2.29 \times 10^{-5}$	$3.68 \times 10^{-10}$

The Fermi level was aligned at  $E_F - E_{\text{HOMO}} = 0.40$  eV for the monomer, 0.39 eV for the dimer and 0.38 eV for the trimer (see text).

absence of a thermally activated hopping mechanism. (As the temperature is increased, eventually electron–electron and electron–phonon scattering will introduce decoherence — the fit between theory and experiment, *vide infra*, suggests that this is not the case for the molecular junctions measured here.) To illustrate this temperature dependence, consider the common case where transport is dominated by a single transmission resonance at energy  $\varepsilon$  of width  $\Gamma \ll k_B T$ , so  $T(E) \approx \Delta \delta(E - \varepsilon)$ , where  $\Delta$  is the area under the resonance. This does not depend on the shape of the resonance, which could have a Lorentzian or Fano lineshape, or be twin peaked in the case of a degeneracy<sup>36</sup>. Equation (1) can then be integrated analytically (see Supplementary Information) to yield

$$I(V, T) \approx \frac{2e}{h} \Delta \exp(-[|\varepsilon - E_F| - |eV/2|]/k_B T) \quad (2)$$

under the conditions  $|\varepsilon - E_F| \gg |eV/2| \gg k_B T$ . Equation (2) indicates that an Arrhenius plot would yield an apparent activation energy of  $(|\varepsilon - E_F| - |eV/2|)$ , as observed in our experiments.

### Ab initio DFT computations

Turning to detailed DFT *ab initio* calculations of  $T(E)$ , we first demonstrate that coherent charge transport can produce low decay factors for the oligo-porphyrin homologous series. Coherent transport has been widely analysed using *ab initio*, non-equilibrium Green's function implementations of the Landauer approach of equation (1). Indeed, there are a growing number of examples of very good correlations between measured molecular conductance and values computed from this approach, particularly when self-energy and screening energy corrections are made to the DFT computed energies<sup>23,36–38</sup>. Our calculations were carried out using our *ab initio* code SMEAGOL<sup>39,40</sup>. An example of one of the simulated systems is shown in Fig. 1b, which shows the butadiyne-linked trimer between gold leads with the three rings lying in one plane. In what follows, results will be presented in the presence of gold adatoms adjacent to the terminal N atoms. Alternative choices are discussed in the Supplementary Information. Figure 3 shows a comparison between our DFT-computed conductances and experimental measurements. In recognition that the free

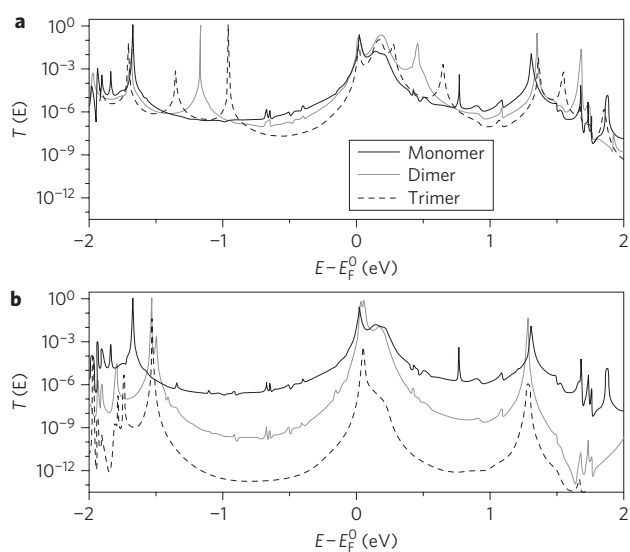


**Figure 4 | Dependence of electron transmission on dihedral angle.** **a, b**, DFT-computed transmission coefficient  $T$  (on a logarithmic scale) versus electron energy for the butadiyne-linked monomer (solid black line), dimer (grey line) and trimer (dashed line) when the angle between the rings of the oligomers is  $0^\circ$  (**a**) and  $90^\circ$  (**b**). (Note that the curves for the monomer are the same in **a** and **b**.)  $E_F^0$  is the value of the Fermi energy predicted by DFT. Other parameters are the same as those used in Fig. 3.

molecule has a low activation barrier for ring rotation<sup>41</sup>, two theoretical cases are shown, in which the porphyrin rings are either all in the same plane, or orientated at  $15^\circ$  to one another, which corresponds to the most stable configuration. Much smaller conductance values are found in the case of orthogonal rings, (Table 1), whereas a reasonably good agreement is obtained for  $0^\circ$  and  $15^\circ$ . A low  $\beta$  value ( $0.04 \text{ \AA}^{-1}$ ) is obtained experimentally, which is similar to the theoretical decay constants for the cases shown in Fig. 3, especially for the  $15^\circ$  case.

In Fig. 4 the transmission curves for molecules **1**, **2** and **3** are plotted for two cases: a planar molecule with a rotation angle of  $0^\circ$  between the rings (Fig. 4a) and the orthogonal case with an angle of  $90^\circ$  between adjacent rings (Fig. 4b). Notice that DFT tends to underestimate the value of the HOMO–LUMO gap, but it is more reliable in predicting relative changes within a homologous series or between different configurations. When the molecule is planar, this gap decreases rather strongly (by  $\sim 0.7$  eV on moving from the monomer to the trimer) as the length of the molecule increases, which gives rise to a low exponential decay of the conductance as a function of length. When the rings are perpendicular, however, the gap changes only slightly (by  $\sim 0.15$  eV). As a consequence of this and the reduction of the width of the resonances, the transmission values in the gap decrease much more rapidly with increasing length when the rings are perpendicular, which gives rise to a rather pronounced exponential decay. Experimental observations<sup>42</sup> indicate that the optical gap decreases by  $\sim 0.3$ – $0.4$  eV on going from monomer to trimer, and this value lies between the values computed here for the planar systems and those with orthogonal rings, respectively. In the light of these experimental and computational observations we conclude the low  $\beta$  values for **1**–**3** arise from a combination of the good conjugation along the oligomers and the length dependence of the HOMO–LUMO gaps.

The finite-temperature conductance was calculated using equation (1) and the transmission coefficient  $T(E)$  obtained from DFT. Because the Fermi energy ( $E_F^0$ ) predicted by DFT is usually unreliable, to compare with experiment we treat the true

Fermi energy  $E_F$  as a free parameter in equation (1) and adjust it to fit the temperature dependence of the experimentally measured conductances. The temperature dependence is significant when the Fermi level sits in the tails of the transmission resonances, but not when it sits on a resonance or in the middle of the HOMO–LUMO gap. This dependence can be clearly seen if the conductance as a function of  $E_F$  is calculated by using equation (1) and a voltage of 0.6 V (shown in Fig. 5 for the monomer).

As can be seen in Table 1, where we use a Fermi energy shift of  $(E_F - E_F^0)$ , which places the Fermi level within the tails of the HOMO (see Supplementary Information), the predicted and measured values for the conductance are rather similar. The Fermi energy chosen to fit the conductance at a given temperature is the single adjustable parameter for each molecule. The fact that the conductance and its temperature dependence are then reproduced so well is compelling evidence for our model. The best agreement between the experimental data and the transport computations is achieved with a Fermi level  $\sim 0.40$  eV above the HOMO for all compounds. This is consistent with previous estimates for porphyrin oligomers similar to **1**–**3**, which point to the Fermi level  $E_F$  lying closer to the HOMO resonance<sup>1</sup>. For the purposes of the comparison, in Table 1 the theoretical conductance data are computed at a representative dihedral angle of  $15^\circ$  (note that the minimum energy is close to  $15^\circ$  dihedral angle for the dimer, see Supplementary Information) as well as  $0^\circ$  and  $90^\circ$ . Although in reality the dimer and trimer may be exploring a wide range of torsional angles, selection of a single angle for the comparison enables us to compute conductance at a high (and time-intensive) computational level. This agreement between theoretical calculations and experiments by fitting just one parameter ( $E_F$ ) demonstrates that the experimental measurements are consistent with phase-coherent transport. The predicted temperature dependence arises from a combination of the energy dependence of the phase-coherent tunnelling of electrons through the effective barrier and the temperature dependence of the Fermi distribution of the injected electron energies. Note that at sufficiently low temperatures, equation (1) yields a temperature-independent conductance, but the required low temperatures are inaccessible in our ambient environment STM.

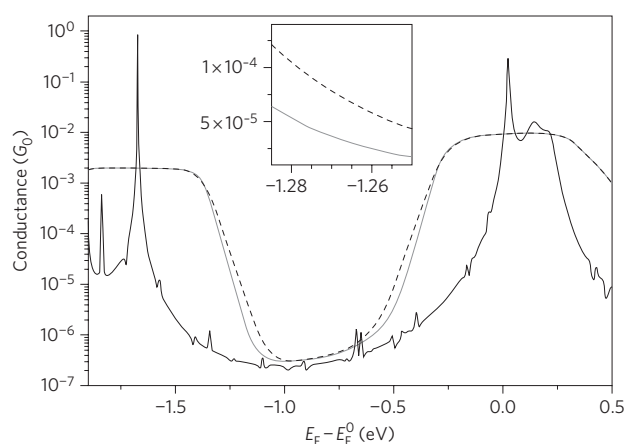


**Figure 5 | Dependence of conductance on temperature.** DFT-computed conductance (on a logarithmic scale) versus  $E_F - E_F^0$ , where  $E_F$  is the true Fermi energy and  $E_F^0$  is given by DFT without adjustment, for the monomer at temperatures of  $25^\circ\text{C}$  (grey line) and  $100^\circ\text{C}$  (dashed line); the black line shows the limit of zero temperature and voltage, which corresponds to the zero-bias transmission  $T$ . Inset: conductance in the region near  $E_F - E_F^0 = -1.27$  eV in more detail (on a linear scale). Other parameters are the same as those used in Fig. 3.

## Conclusions

We have shown experimentally that the single oligo-porphyrin molecular electrical junctions exhibit significant temperature dependence. A very shallow decay of conductance with length is also observed. Naively, both of these factors might seem to point to an incoherent thermally assisted hopping mechanism. However, the increasing temperature dependence in the sequence monomer–dimer–trimer goes against such an inference; furthermore, we have shown that transport in these molecular junctions is convincingly described by a theory based on phase-coherent electron tunnelling using  $E_F$  as a single adjustable parameter.

## Methods

The  $I(s)$  method has been used to determine molecular conductance and its dependence on temperature<sup>31</sup>. In the  $I(s)$  technique, current  $I$  is recorded and the tip is rapidly retracted ( $s$  = distance) from a given set-point current ( $I_0$ ) following temporarily disabling the feedback loop. The set-point parameters can be used to control the initial distance between tip and substrate, and for a given bias voltage higher set-point current ( $I_0$ ) results in a closer initial approach of the tip to the substrate. If molecules become attached between the gold STM tip and the gold substrate at the start of an  $I(s)$  retraction sweep, they are then pulled up in the junction until the molecular bridge is broken. This results in characteristic current plateaux when molecular wires bridge the gap between the tip and substrate, examples of which are shown in Fig. 2a (inset). However, in the absence of molecular bridge formation, the current simply decreases exponentially with separation. The key difference between the  $I(s)$  technique and the *in situ* break-junction method<sup>28,43,44</sup>, which also uses an STM as the method of junction formation, is that direct metal-to-metal contact between tip and substrate is avoided, with molecular junctions being formed when the STM tip is brought sufficiently close to the surface covered by the target molecules and then withdrawn while the junction current is measured. Both techniques, however, use a similar method of analysis in which current–distance curves, or current steps in the current–distance curves, are statistically analysed in a histogram representation. Many resulting current–distance traces are recorded, and those that show discernible plateaux are collected together in histogram plots of conductance values. The occurrence of plateaux in the collected  $I$ – $s$  curves results in peaks in the conductance histograms. The lowest conductance peaks are attributed to single molecular junctions. All  $I(s)$  measurements were conducted in air. For a given set-point current and bias voltage, typically 2,000–4,000 events were made, but only curves showing current steps associated with the formation of molecular bridges were recorded. These occurred during 10–20% of retraction events, and curves that did not exhibit such features (for example, showing exponential decay) were not used in the histogram analysis.

DFT-based transport calculations were carried out using our *ab initio* code SMEAGOL<sup>39,40</sup>, which uses a combination of the SIESTA implementation of DFT<sup>45</sup> and scattering theory. SIESTA uses norm-conserving pseudopotentials to eliminate the core electrons and linear combinations of pseudo-atomic orbitals to calculate the single-particle wavefunctions. The underlying mean-field DFT-derived Hamiltonian is then used to compute phase-coherent, elastic scattering properties of the molecule connected to gold electrodes. The choice of the same large gold contacts in each computation made the simulations particularly lengthy (the total number of atoms could be as high as 588 for the butadiyne-linked trimer and up to 1,026 for the tilted monomer (see Supplementary Information), and we also had to include all valence states,  $s$  and  $d$ , in the gold atoms as including only  $s$  states gave incorrect charge transfer between the molecule and the surface). The Au–N binding distance was set to 2.0 Å, which was obtained by optimizing the distance between the N terminating atom of a monomer molecule and the gold adatom on top of a gold slab made of four gold layers, using the same parameters that were used in the transport calculation. The gold adatom on the surface was also relaxed. Further details are given in the Supplementary Information.

Received 17 May 2011; accepted 15 June 2011;  
published online 31 July 2011

## References

- Sedghi, G. *et al.* Single molecule conductance of porphyrin wires with ultralow attenuation. *J. Am. Chem. Soc.* **130**, 8582–8583 (2008).
- Kang, B. K. *et al.* Length and temperature dependence of electrical conduction through dithiolated porphyrin arrays. *Chem. Phys. Lett.* **412**, 303–306 (2005).
- Yoon, D. H. *et al.* Electrical conduction through linear porphyrin arrays. *J. Am. Chem. Soc.* **125**, 11062–11064 (2003).
- Kiguchi, M., Takahashi, T., Kanehara, M., Teranishi, T. & Murakoshi, K. Effect of end group position on the formation of a single porphyrin molecular junction. *J. Phys. Chem. C* **113**, 9014–9017 (2009).
- Winters, M. U. *et al.* Probing the efficiency of electron transfer through porphyrin-based molecular wires. *J. Am. Chem. Soc.* **129**, 4291–4297 (2007).
- Imahori, H. *et al.* Modulating charge separation and charge recombination dynamics in porphyrin fullerene linked dyads and triads: Marcus-normal versus inverted region. *J. Am. Chem. Soc.* **123**, 2607–2617 (2001).
- Guldi, D. M. *et al.* A molecular tetrad allowing efficient energy storage for 1.6 s at 163 K. *J. Phys. Chem. A* **108**, 541–548 (2004).
- Grozema, F. C., Houarner-Rassin, C., Prins, P., Siebbeles, L. D. A. & Anderson, H. L. Supramolecular control of charge transport in molecular wires. *J. Am. Chem. Soc.* **129**, 13370–13371 (2007).
- Leggett, G. J. *Surface Analysis — The Principal Techniques* 2nd edn (eds Vickerman, J. C. & Gilmore, I. S.) Ch. 9 (Wiley, 2009).
- Cuevas, J. C. & Scheer, E. *Molecular Electronics: An Introduction to Theory and Practice* (World Scientific, 2010).
- Choi, S. H., Kim, B. & Frisbie, C. D. Electrical resistance of long conjugated molecular wires. *Science* **320**, 1482–1486 (2008).
- Choi, S. H. *et al.* Transition from tunneling to hopping transport in long, conjugated oligo-imine wires connected to metals. *J. Am. Chem. Soc.* **132**, 4358–4368 (2010).
- Selzer, Y., Cabassi, M. A., Mayer, T. S. & Allara, D. L. Thermally activated conduction in molecular junctions. *J. Am. Chem. Soc.* **126**, 4052–4053 (2004).
- Poot, M. *et al.* Temperature dependence of three-terminal molecular junctions with sulfur end-functionalized teracyclohexylidenes. *Nano Lett.* **6**, 1031–1035 (2006).
- Haiss, W. *et al.* Thermal gating of the single molecule conductance of alkanedithiols. *Faraday Discuss.* **131**, 253–264 (2006).
- Martin, S. *et al.* Influence of conformational flexibility on single-molecule conduction in nano-electrical junctions. *J. Phys. Chem. C* **113**, 18884–18890 (2009).
- Li, X. L. *et al.* Conductance of single alkanedithiols: conduction mechanism and effect of molecule–electrode contacts. *J. Am. Chem. Soc.* **128**, 2135–2141 (2006).
- Li, X. L. *et al.* Thermally activated electron transport in single redox molecules. *J. Am. Chem. Soc.* **129**, 11535–11542 (2007).
- Diez-Perez, I. *et al.* Gate-controlled electron transport in coronenes as a bottom-up approach towards graphene transistors. *Nature Commun.* **1**, 3 (2010).
- Chanteau, S. H. & Tour, J. M. Synthesis of potential molecular electronic devices containing pyridine units. *Tetrahedron Lett.* **42**, 3057–3060 (2001).
- Flatt, A. K. *et al.* Synthesis and testing of new end-functionalized oligomers for molecular electronics. *Tetrahedron* **59**, 8555–8570 (2003).
- Quek, S. Y. *et al.* Mechanically controlled binary conductance switching of a single-molecule junction. *Nature Nanotech.* **4**, 230–234 (2009).
- Wang, C. S. *et al.* Oligoene single molecule wires. *J. Am. Chem. Soc.* **131**, 15647–15654 (2009).
- Zhou, X. S. *et al.* Single molecule conductance of dipyrindines with conjugated ethene and nonconjugated ethane bridging group. *J. Phys. Chem. C* **112**, 3935–3940 (2008).
- Li, X. L. *et al.* Controlling charge transport in single molecules using electrochemical gate. *Faraday Discuss.* **131**, 111–120 (2006).
- Kushmerick, J. G., Whitaker, C. M., Pollack, S. K., Schull, T. L. & Shashidhar, R. Tuning current rectification across molecular junctions. *Nanotechnology* **15**, S489–S493 (2004).
- Li, C. *et al.* Electrochemical gate-controlled electron transport of redox-active single perylene bisimide molecular junctions. *J. Phys. Condens. Matter* **20**, 374122 (2008).
- Xu, B. Q. & Tao, N. J. Measurement of single-molecule resistance by repeated formation of molecular junctions. *Science* **301**, 1221–1223 (2003).
- Haiss, W. *et al.* Precision control of single-molecule electrical junctions. *Nature Mater.* **5**, 995–1002 (2006).
- Haiss, W. *et al.* Measurement of single molecule conductivity using the spontaneous formation of molecular wires. *Phys. Chem. Chem. Phys.* **6**, 4330–4337 (2004).
- Haiss, W. *et al.* Redox state dependence of single molecule conductivity. *J. Am. Chem. Soc.* **125**, 15294–15295 (2003).
- Gol'dshtrakh, M. A., Dorofeev, S. G., Ishchenko, A. A., Kiselev, Y. M. & Kononov, N. N. A comparative analysis of the influence of photo- and thermal activation on the sensor properties of cobalt(II) etioporphyrin films. *Russian J. Phys. Chem. A* **83**, 1775–1780 (2009).
- Takahashi, K., Horino, K., Komura, T. & Murata, K. Photovoltaic properties of porphyrin thin-films mixed with o-chloranil. *Bull. Chem. Soc. Jpn* **66**, 733–738 (1993).
- Banerjee, P. *et al.* Plasmon-induced electrical conduction in molecular devices. *ACS Nano* **4**, 1019–1025.
- He, J., Forzani, E. S., Nagahara, L. A., Tao, N. J. & Lindsay, S. Charge transport in mesoscopic conducting polymer wires. *J. Phys. Condens. Matter* **20**, 374120 (2008).
- Neaton, J. B., Hybertsen, M. S. & Louie, S. G. Renormalization of molecular electronic levels at metal–molecule interfaces. *Phys. Rev. Lett.* **97**, 216405 (2006).
- Quek, S. Y. *et al.* Amine-gold linked single-molecule circuits: experiment and theory. *Nano Lett.* **7**, 3477–3482 (2007).
- Kristensen, I. S., Mowbray, D. J., Thygesen, K. S. & Jacobsen, K. W. Comparative study of anchoring groups for molecular electronics: structure and conductance of Au–S–Au and Au–NH<sub>2</sub>–Au junctions. *J. Phys. Condens. Matter* **20**, 374101 (2008).

39. Rocha, A. R. *et al.* Spin and molecular electronics in atomically generated orbital landscapes. *Phys. Rev. B* **73**, 085414 (2006).
40. Rocha, A. R. *et al.* Towards molecular spintronics. *Nature Mater.* **4**, 335–339 (2005).
41. Winters, M. U. *et al.* Photophysics of a butadiyne-linked porphyrin dimer: influence of conformational flexibility in the ground and first singlet excited state. *J. Phys. Chem. C* **111**, 7192–7199 (2007).
42. Taylor, P. N. *et al.* Conjugated porphyrin oligomers from monomer to hexamer. *Chem. Commun.* 909–910 (1998).
43. Tao, N. J. Electron transport in molecular junctions. *Nature Nanotech.* **1**, 173–181 (2006).
44. Venkataraman, L., Klare, J. E., Nuckolls, C., Hybertsen, M. S. & Steigerwald, M. L. Dependence of single-molecule junction conductance on molecular conformation. *Nature* **442**, 904–907 (2006).
45. Soler, J. M. *et al.* The SIESTA method for *ab initio* order-*N* materials simulation. *J. Phys. Condens. Matter* **14**, 2745–2779 (2002).

### Acknowledgements

This work was supported by the Engineering and Physical Sciences Research Council (EPSRC; grant nos EP/D07665X/1, EP/D076552/1 and GR/S84064/01), QinetiQ, the Department of Trade and Industry, the Royal Society and the Northwest Regional

Development Agency. The authors thank the EPSRC mass spectrometry service (Swansea) for mass spectra. V.G-S. acknowledges his Ramón y Cajal position and his previous Juan de la Cierva position from the Ministerio de Ciencia e Innovación, Spain. S.M. acknowledges his Juan de la Cierva position from the Ministerio de Ciencia e Innovación, Spain. The NWGrid is thanked for computing resources.

### Author contributions

G.S. performed experimental conductance measurements and analysed the data, in part with the assistance of S.M. V.G-S. performed DFT computations and analysed computational data. L.J.E. synthesized and chemically characterized the compounds. M.E. originated the analytical model and further developed it in consultation with C.J.L. N.B. performed supporting STM characterization measurements and contributed to numerical calculations of the Lorentzian model. G.S., V.G-S., H.L.A., C.J.L., S.J.H., M.E. and R.J.N. were involved in writing the manuscript and supporting information. H.L.A., C.J.L., D.B., S.J.H., M.E., E.M. and R.J.N. provided supervision at the different sites.

### Additional information

The authors declare no competing financial interests. Supplementary information accompanies this paper at [www.nature.com/naturenanotechnology](http://www.nature.com/naturenanotechnology). Reprints and permission information is available online at <http://www.nature.com/reprints>. Correspondence and requests for materials should be addressed to H.L.A., C.J.L. and R.J.N.